Monatshefte für Chemie 136, 519–536 (2005)
DOI 10.1007/s00706-004-0224-4

Monatshefte für Chemie
Chemical Monthly
Printed in Austria

ESR and ENDOR Investigations on Various *Wurster*'s Radical Cations in Solution. Experimental Results, Theoretical *ab initio*, and DFT Calculations

Günter Grampp[1,*], **Anne-Marie Kelterer**[1], **Stephan Landgraf**[1], **Michael Sacher**[1], **Dominique Niethammer**[2], **João P. Telo**[3], **Rui M. B. Dias**[3], and **Abel J. S. C. Vieira**[4]

[1] Graz University of Technology, Institute of Physical and Theoretical Chemistry, A-8010 Graz, Austria
[2] Free University of Berlin, Institute of Organic Chemistry, D-14195 Berlin, Germany
[3] Instituto Superior Tecnico, Química Organica, P-1096 Lisbon, Portugal
[4] Universidade de Nova Lisboa, Departmento de Química, P-2825-114 Monte de Caparica, Portugal

Received February 6, 2004; accepted (revised) May 23, 2004.
Published online January 31, 2005

Summary. ESR and ENDOR spectra are reported of several symmetrical substituted *N*,*N*,*N*′,*N*′-tetraalkyl-*p*-phenylenediamine radical cations in solution. Different *N*,*N*′-alkyl substituted *para*-phenylenediamines, like the ethyl, *n*-propyl, and *iso*-propyl derivative are compared with the parent *N*,*N*,*N*′,*N*′-tetramethyl-*p*-phenylenediamine (*Wurster*'s Blue Cation). *N*,*N*,*N*′,*N*′-Tetrabenzyl-*p*-phenylenediamine, 1,4-dipyrrolidinylbenzene, and *N*,*N*′-bis[4-(dimethylamino)phenyl]piperazine are additionally investigated. Experimental and calculated hyperfine coupling constants are compared. Characteristic UV-VIS data and redox potentials in acetonitrile are reported, together with the syntheses of the compounds.

Keywords. ESR; ENDOR; *Wurster*'s radical cations; Hyperfine coupling constants; *Ab initio*; AM1; DFT; *B3LYP*; Spin density calculations.

Introduction

More than 100 years ago the persistent one-electron oxidation products of *p*-phenylenediamines and their derivatives have been discovered by *C. Wurster* [1].

* Corresponding author. E-mail: grampp@ptc.tugraz.at

The radical character of these compounds has been recognized by use of magnetic balance measurements much later [2], the coloured radicals have been named in the literature according to their discoverer as *Wurster*'s cations, especially the highly stable semiquinone radical cation of *N*,*N*,*N*′,*N*′-tetramethyl-*p*-phenylenediamine (*Wurster*'s Blue), and the radical cation of *N*,*N*-dimethyl-*p*-phenylenediamine (*Wurster*'s Red).

p-Phenylenediamines found a wide range of applications from industrial, commercial, and scientific points of view. One of the important industrial applications is their utilization as film developers, especially as coupling components in the developing process of color films and slides [3]. *Weissman et al.* [4–6] published the first papers on ESR investigations of *Wurster*'s Blue and *Wurster*'s Red radical cations. Other early reports were given by *Hausser* [7, 8]. The first detailed interpretation of the complex ESR-spectrum of *N*,*N*,*N*′,*N*′-tetramethyl-*p*-phenylenediamine was reported by *Bolton et al.* [9] and later in the textbook of *Wertz* and *Bolton* [10, 11], who used it as an ESR-standard for magnetic field calibration and for *g*-factor measurements. The number of papers dealing with ESR data of the radical cation of *N*,*N*-dimethyl-*p*-phenylenediamine (*Wurster*'s Red Cation) is relatively small [12–14]. Slightly different results are reported on the hyperfine coupling constants of this radical cation [15, 16]. *Grampp* and *Stiegler* [12] gave a detailed analysis of the corresponding ESR spectrum based on specific deuteration.

A degeneration by chance is reported for the nitrogen and the methyl proton coupling constants $(a^{N} = 3a^{H}_{Me})$ of the 2,3,5,6-tetramethyl-*p*-phenylenediamine radical cation [12, 17, 18]. To our knowledge, the ESR spectrum of the *N*,*N*,*N*′,*N*′-tetraethyl-*p*-phenylenediamine radical cation is reported only in three publications [12, 19, 20]. The published ESR coupling constants in Refs. [12] and [19] correlate well with our ESR and ENDOR results, whereas in Ref. [20] identical coupling constants are given for different alkyl substituents (R = ethyl, *n*-propyl, *n*-butyl). This is probably due to poor spectral resolution.

From the higher derivatives of the *sym*-*N*,*N*,*N*′,*N*′-tetraalkyl substituted *Wurster*'s cations only very few ESR-reports exist [20–23]. Up to now no detailed ENDOR-investigations have been reported. The aim of this paper is to present detailed ESR and ENDOR data of higher substituted tetraalkyl-*p*-phenylenediamines together with UV-VIS data, redox properties, and detailed quantum chemical spin density calculations. We report on the radical cations of *N*,*N*,*N*′,*N*′-tetraethyl-*PPD* (*TEPPD*), *N*,*N*,*N*′,*N*′-tetra-*n*-propyl-*PPD* (*TPPPD*), *N*,*N*,*N*′,*N*′-tetra-*iso*-propyl-*PPD* (*TiPPPD*), *N*,*N*,*N*′,*N*′-tetrabenzyl-*PPD* (*TBzPPD*), 1,4-dipyrrolidinylbenzene (*DPB*), and for comparison on *N*,*N*,*N*′,*N*′-tetramethyl-*p*-phenylenediamine (*TMPPD*). Additionally we report on the *N*,*N*′-bis[4-(dimethylamino)phenyl]piperazine *BDMAP* radical cation, a compound recently described by *Nelsen et al.* [24]. Structures are shown in Scheme 1.

The alkyl substituted compounds have, to the best of our knowledge, not yet been investigated by computational methods. Therefore, various quantum chemical investigations have been performed at appropriate levels. The complete conformational analyses done with the semiempirical AM1 method include *TEPPD* and *TPPPD* with respect to the conformers which are populated under our experimental conditions at room temperature. For *TBzPPD* and *DPB* the global minimum of

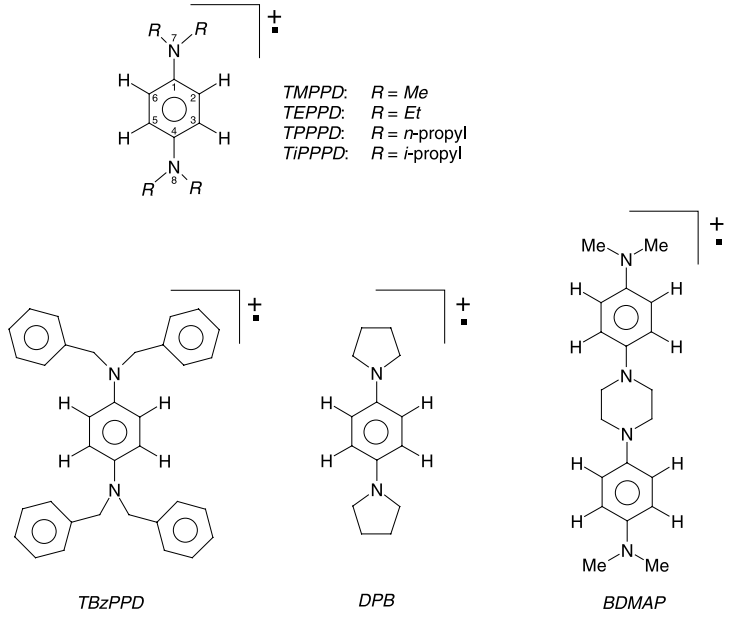

Scheme 1

TEPPD was the starting point in our study. Final conformational analyses done by the density functional approach using the *B3LYP* functional with the 6-31G* basis set are presented, leading to calculated spin densities which are correlated with the experimental hyperfine coupling constants.

Results and Discussion

Figures 1–5 show the experimental ESR and ENDOR spectra of the radical cations from *TEPPD*, *TPPPD*, *TiPPPD*, *TBzPPD*, *DPB*, and *N*,*N*′-bis[4-(dimethylamino)phenyl]piperazine (*BDMAP*), together with the corresponding simulations. All ESR hyperfine coupling constants obtained are listed in Tables 1–7. As expected, only slight changes in the hyperfine coupling constants occur compared to *Wurster*'s Blue cation of *TMPPD*, depending on the nature of the substituents. The ESR nitrogen coupling a^{N} decreases from 0.705 mT (*TMPPD*, *R* = *Me*, Table 1) to 0.696 mT for the ethyl substituent (Table 2) and then increases again to 0.715 mT for both, the *n*-propyl (Table 3) and the *i*-propyl (Table 4) compound. The coupling constants of the tetrabenzyl substituted radical show values similar to the other alkylsubstituted compounds. An interesting change in the relation of the nitrogen coupling constant, a^{N}, and the adjacent hydrogen coupling is observed in the *DPB* radical cation compared to the other radical cations. Unhindered rotation of the methyl groups in *TMPPD* gave a ratio of R = 1.04 for a^{N}/a^{H}_{Me}, indicating a planar geometry with freely rotating CH_3-groups. Changing from methyl to methylene groups, as per *TEPPD*, *TPPPD*, *TBzPPD*, this ratio increases to a mean value of R = 1.85. The strong steric hindrance in *TiPPPD* increases R to 7.15, as also shown by *Bock et al.* [28].

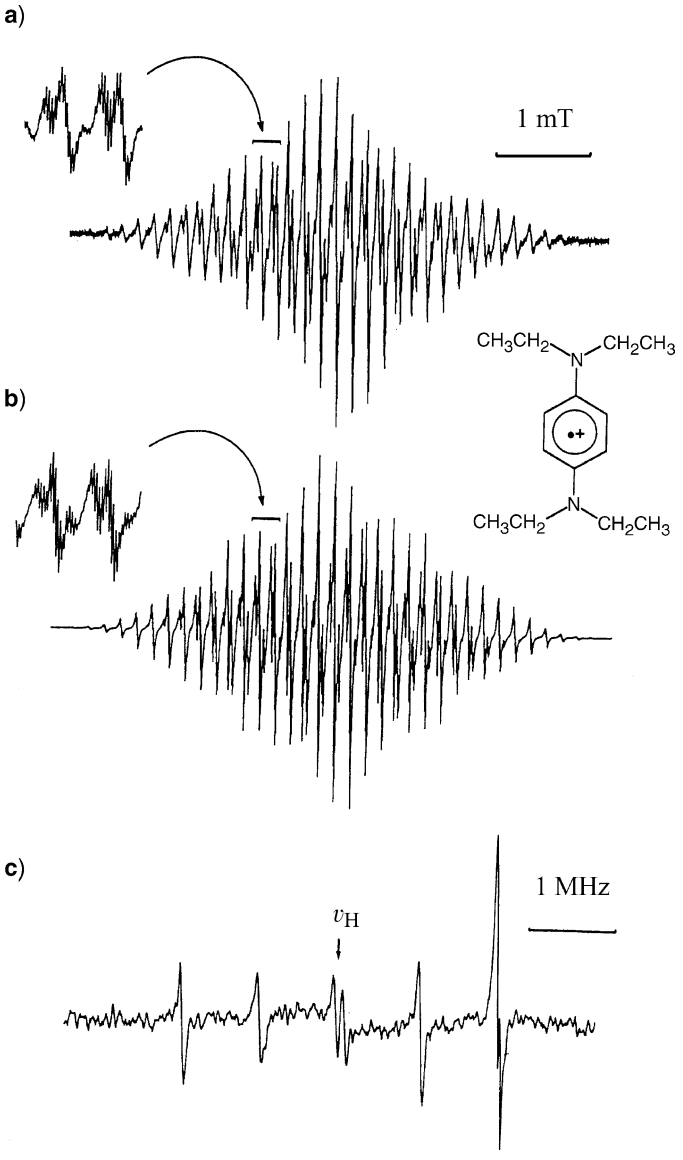

Fig. 1. a) Experimental CW-ESR spectrum of the *N*,*N*,*N*′,*N*′-tetraethyl-*p*-phenylenediamine radical cation in H_2O at $T = 298$ K; b) simulated spectrum, inserts: enlargements of 0.3 mT; c) ENDOR-spectrum in glycerol/H_2O (3:1 v/v) at $T = 298$ K

This ratio changes to values lower than one for the less flexible radical cations of *DPB* and *BDMAP*, where different ring systems adjacent to the nitrogen atoms are present. R = 0.70 and 0.94 are the $a^N/a^H_{-CH_2-}$-ratios, respectively.

The coupling constants of the aromatic protons remain nearly constant. These values cover a small range from 0.189 to 0.199 mT. According to the strong out-of-plane arrangement of the isopropyl groups, two types of β-protons with slightly different couplings are found, both experimentally and theoretically, see Table 4. $a_1^{H\beta} = 0.100$ mT and $a_2^{H\beta} = 0.075$ mT are the corresponding

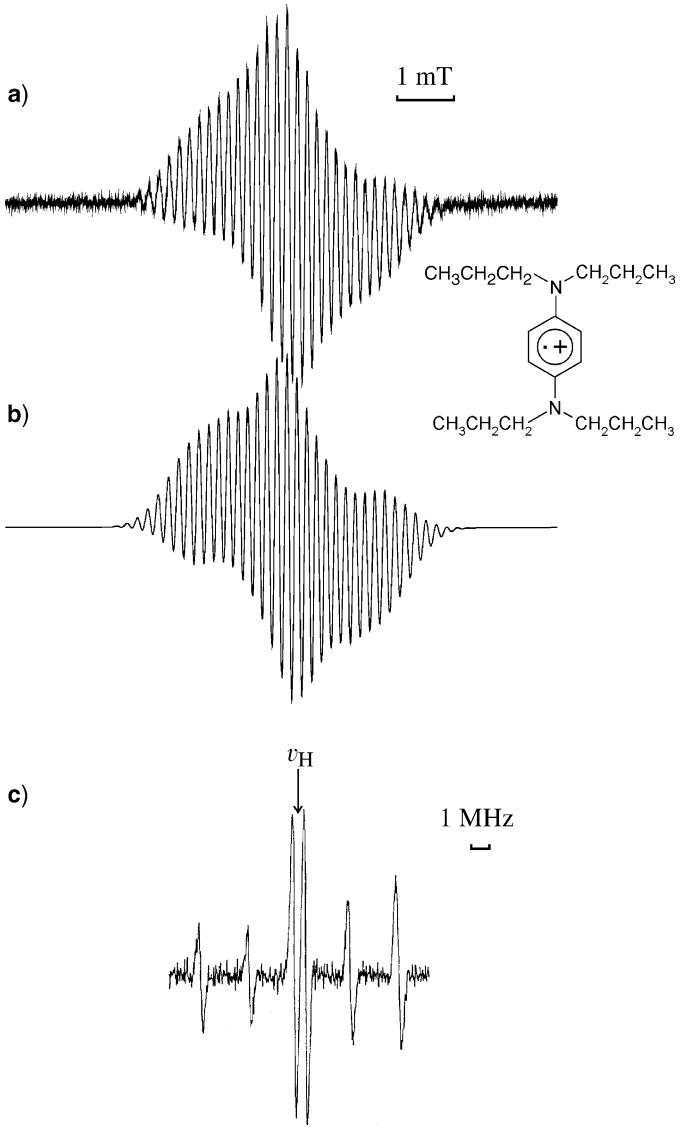

Fig. 2. a) Experimental CW-ESR spectrum of the *N*,*N*,*N*′,*N*′-tetra-*n*-propyl-*p*-phenylenediamine radical cation in 2-propanol/*DMSO* (1:1 *v*/*v*) at $T = 280\,\mathrm{K}$; b) simulated spectrum; c) ENDOR-spectrum in 2-propanol/*DMSO* (1:1 *v*/*v*) at $T = 280\,\mathrm{K}$

proton coupling constants. Values found for the γ-protons are extremely small, as normally reported for such type of protons [29, 30]. The assignment of the hfc-constant of the *N*,*N*′-bis[4-(dimethylamino)phenyl]piperazine radical cation is given in Table 7. The hyperfine pattern shows two nearly equivalent nitrogen couplings, four equivalent aromatic protons, and ten nearly equivalent protons from two methyl and two methylene groups. These values clearly indicate that the unpaired electron is localized on one *p*-phenylenediamine subunit.

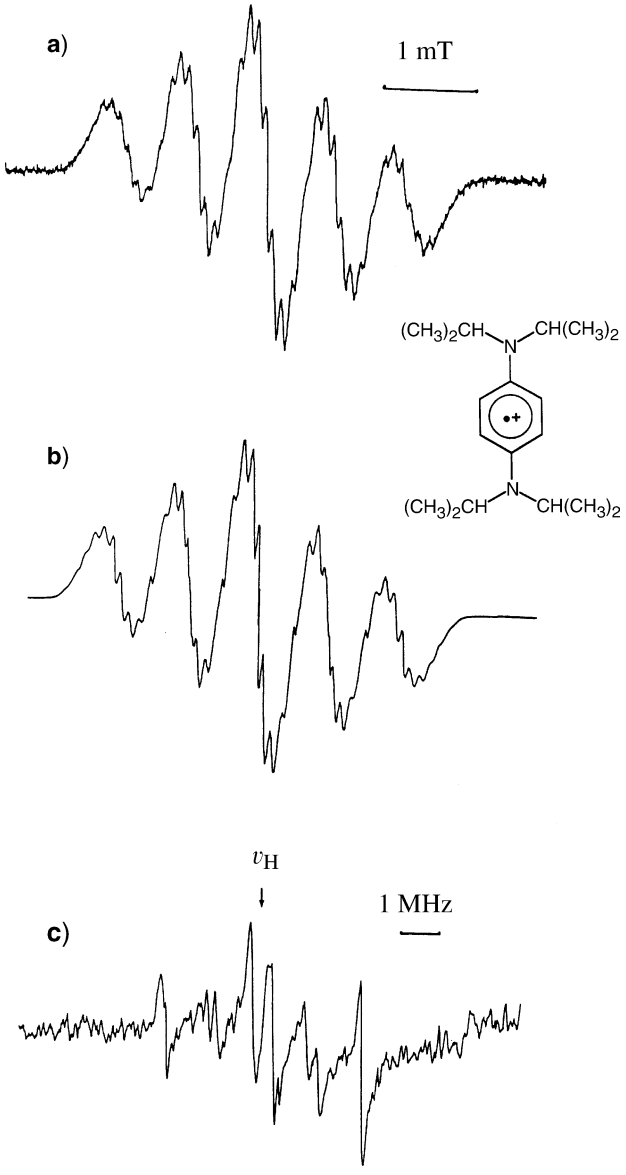

Fig. 3. a) Experimental CW-ESR spectrum of the *N*,*N*,*N*′,*N*′-tetra-*iso*-propyl-*p*-phenylenediamine radical cation in H_2O at $T = 298$ K; b) simulated spectrum; c) ENDOR-spectrum in glycerol/H_2O (3:1 v/v) at $T = 298$ K

The cyclic voltamogramms of all compounds clearly show two separated reversible oxidation steps. Redox potentials of the first and second oxidation steps are given in Table 10. Whereas the first oxidation potentials, $E_{ox}^{(1)}$, are similar for *TMPPD* and *TiPPPD* and for TEPPD and *TPPPD*, the second oxidation steps for the quinonediimine are nearly identical for these four compounds and independent of the substituents on *N*. The reason for this may be that these radical cations as well as the corresponding quinonediimines are completely planar, as indicated

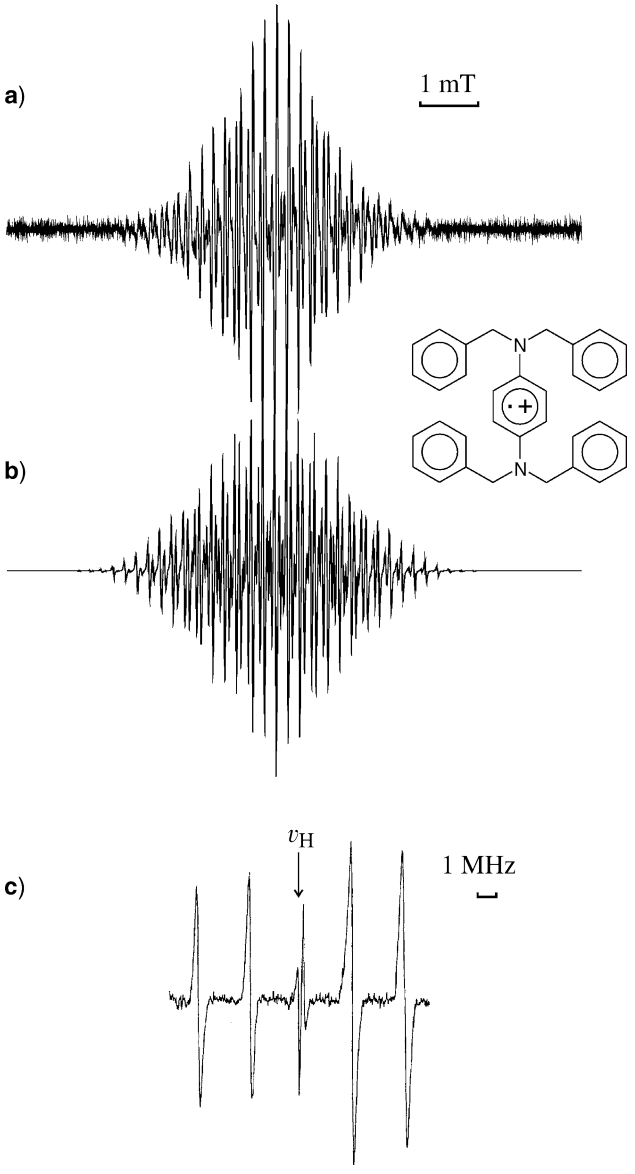

Fig. 4. a) Experimental CW-ESR spectrum of the *N*,*N*,*N*′,*N*′-tetrabenzyl-*p*-phenylenediamine radical cation in 2-propanol/*DMSO* (1:1 *v*/*v*) at $T = 300$ K; b) simulated ESR-spectrum; c) ENDOR-spectrum in 2-propanol/*DMSO* (1:1 *v*/*v*) at $T = 300$ K

by both ESR results and theoretical calculations. The oxidation potentials decrease from *TMPPD*, TEPPD to *TPPPD*, revealing the increasing electron releasing effect in the homologous series of substituents: methyl, ethyl, and propyl. A *Hammett* plot with these three compounds is linear. The redox potential of *TiPPPD* does not fall on such a *Hammett* plot, its potential increases to -295 mV, indicating the lower stability of this radical cation. Again its steric hindrance may be the reason for such a behaviour. An X-ray structure for the diprotonated *TiPPPD* H_2^{2+} is reported in the literature [28], the two isopropyl groups attached to each nitrogen

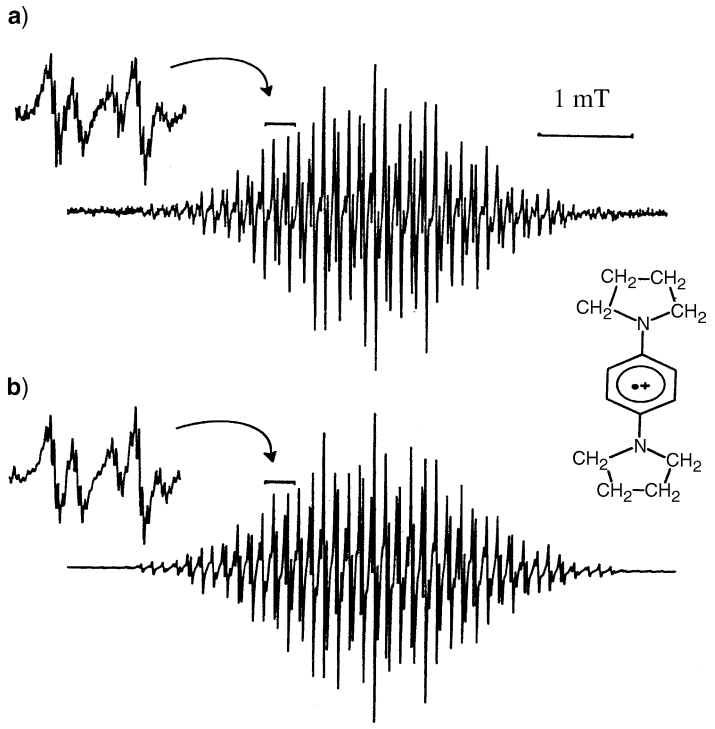

Fig. 5. a) Experimental CW-ESR spectrum of the 1,4-dipyrrolidinylbenzene radical cation in H_2O at $T = 298$ K; b) simulated spectrum, inserts: enlargements of 0.3 mT region

Table 1. Experimental and theoretical hfc-constants [mT] of the $TMPPD^{\bullet+}$; geometries of the structure in Ref. [25] were reoptimized with the *B3LYP*/6-31G* method; the *Fermi* contact analysis is made by the methods listed

$TMPPD^{\bullet+}$	ESR	U*B3LYP*/6-31G*	U*B3LYP*/ESR-II
a^N	0.705[a] 0.7051[b]	0.652	0.552
a^H_{arom}	0.199[a] 0.1989[b]	−0.19	−0.185
$a^H_{CH_3}$	0.677[a] 0.6773[b]	0.731	0.781

[a] In abs. methanol at $T = 293$ K, Ref. [12]; [b] in abs. ethanol at $T = 296$ K, Ref. [10]

atom are twisted by 56 and 77° out of the plane of the benzene ring. A different behaviour is also found for the potentials of *TBzPPD* and *DPB*. *DPD* is a somewhat different system since the alkyl groups are fixed there in a five-membered ring. The first oxidation step of *DPB* is identical to that of *TPPPD*, whereas the second oxidation is performed easier compared with *TPPPD*. *TBzPPD* shows the highest $E^{(1)}_{ox}$-value, −120 mV *vs.* Fc/Fc^+, and also the highest $E^{(2)}_{ox}$, 525 mV *vs.* Fc/Fc^+, for forming the corresponding quinonediimine dication.

Table 2. Experimental and theoretical hfc-constants [mT] of $TEPPD^{+\bullet}$; the calculated hfc-constants are the result of *Boltzmann* distribution at room temperature including the DFT data from Table 8; *Fermi* contact analysis is made with the methods listed

$TEPPD^{+\bullet}$	ESR	ENDOR	U*B3LYP*/6-31G*	U*B3LYP*/ESR-II
a^{N}	0.688[a] 0.696[b]	–	0.665	0.565
a^{H}_{arom}	0.185[a] 0.198[b] 0.188[c]	0.1967[d] 0.197[b]	−0.188	−0.184
$a^{H\beta}$	0.369[a] 0.372[b] 0.376[c]	0.3841[d] 0.379[b]	0.371	0.308 0.475
$a^{H\gamma}$	0.010[a] 0.010[b] 0.0096[c]	0.0105[d] 0.010[b]	−0.008	−0.005

[a] In abs. methanol at $T = 293$ K, Ref. [12]; [b] in 2-propanol/*DMSO* mixture at $T = 280$ K; [c] in H_2O at $T = 298$ K; [d] in glycerol/H_2O at $T = 298$ K

Table 3. Experimental and calculated hfc-constants [mT] of the $TPPPD^{+\bullet}$; the calculated hfc-constants are the result of *Boltzmann* distribution at room temperature including the DFT data from Table 9; *Fermi* contact analysis is made with the method listed

$TPPPD^{+\bullet}$	ESR	ENDOR	U*B3LYP*/6-31G*
a^{N}	0.715[a] 0.692[b] 0.697[c]	0.695[a]	0.664
$a^{H}_{arom.}$	0.199[a] 0.181[b] 0.194[c]	0.194[a]	−0.185
$a^{H\beta}$	0.377[a, c] 0.380[b]	0.378[a]	0.374
$a^{H\gamma}$	0.027[a] 0.028[b] 0.0203[c]	0.022[a]	−0.036
$a^{H\delta}$	–	–	0.022

[a] In 2-propanol/*DMSO* at $T = 290$ K; [b] in methanol at $T = 265$ K; [c] in H_2O at $T = 298$ K

Theoretical Investigations of Spin Densities

Methods

The isotropic hyperfine coupling constants depend strongly on the geometry and especially the bond lengths of the radicals. Based on a paper of *Gescheidt et al.* [31] that compares semiempirical *Hartree-Fock* and density functional methods for

Table 4. Experimental and calculated hfc-constants [mT] of the *TiPPPD*$^{+\bullet}$; the *Fermi* contact analysis is done for the all-t-conformer with the method listed

TiPPPD$^{+\bullet}$	ESR	ENDOR	U*B3LYP*/6-31G*
a^{N}	0.715[a] 0.715[b]	0.714[a]	0.700
$a^{H}_{arom.}$	0.189[a] 0.177[b]	0.187[a] 0.187[c]	−0.158
$a^{H\beta}_{1}$	0.100[a] 0.101[b]	0.100[a] 0.104[c]	0.163
$a^{H\beta}_{2}$	0.075[a]	0.075[a] 0.085[c]	−0.024
$a^{H\gamma}$	0.016[a]	0.017[a, c]	–

[a] In 2-propanol/*DMSO* at $T = 280$ K; [b] in methanol at $T = 267$ K; [c] in glycerol/H_2O at $T = 298$ K

Table 5. Experimental hfc-constants [mT] of the *TBzPPD*$^{+\bullet}$

TBzPPD$^{+\bullet}$	ESR	ENDOR
a^{N}	0.672[b] 0.662[c]	–
$a^{H}_{arom.}$	0.193[b] 0.197[c]	0.188[a]
$a^{H\beta}$	0.388[b] 0.389[c]	0.390[a]
a^{H}_{phenyl}	0.007[b]	0.014[a]

[a] In 2-propanol/*DMSO* at $T = 300$ K; [b] in 2-propanol/*DMSO* at $T = 280$ K; [c] in methanol at $T = 265$ K

Table 6. Experimental and calculated hfc-constants [mT] of the *DPB*$^{+\bullet}$; the *Fermi* contact analysis is done for the global minimum with the method listed

DPB$^{+\bullet}$	ESR	ENDOR	U*B3LYP*/6-31G*
a^{N}	0.682[a] 0.687[b]	0.686[a]	0.648
$a^{H}_{arom.}$	0.201[a] 0.201[b]	0.200[a]	–
$a^{H\beta}$	0.975[a] 0.959[b]	0.966[a]	–
$a^{H\gamma}$	0.017[a] 0.014[b]	0.015[a]	–

[a] In 2-propanol/*DMSO* at $T = 270$ K; [b] in H_2O at $T = 298$ K

Table 7. Experimental hfc-constants [mT] of the *N,N′*-bis[4-(dimethylamino)phenyl]piperazine radical cation

$BDMAP^{+\bullet}$	ESR
a^{N}	0.703[a]
$a^{H}_{CH_3,-CH_2-}$	0.750[a]
$a^{H}_{arom.}$	0.189[a]

[a] In methanol/ethanol mixture (1:4 *v*/*v*) at $T = 268$ K

Table 8. Relative AM1 and *B3LYP*/6-31G* energies (in kJ/mol) and hyperfine coupling constants (mT) of the *TEPPD* radical cation; the DFT conformers were used for the *Boltzmann* distribution; the *B3LYP*/6-31G* absolute energy of the global minimum is −657.2386734 a.U.; the dihedral angles of the ethyl unit are gauche, $g \sim 60$ degree, $g' \sim -60$ degree and trans, $t \sim 180$ degree for the rotation around the $-CH_2-CH_3$ bond

Structure	$ggg'g'$	$gggg$	$gggg'$	$ggg'g'$	$gg'gg'$
degeneration	4	2	8	4	4
E_{rel}(AM1)	0.0	0.12	1.63	3.13	3.26
E_{rel}(DFT)	0.0	0.10	4.60	8.90	9.36
Boltzmann distribution	50.6%	25.1%	17%	6.1%	1.2%
$a(H_{ar})$	−0.189	−0.186	−0.187	−0.187	−0.187
$a(H\alpha)$	0.294 (4H)	0.307 (4H)	0.303 (3H)	0.522 (4H)	0.339 (4H)
	0.448 (4H)	0.432 (4H)	0.443 (3H)	0.222 (4H)	0.224 (4H)
			0.576 (1H)		
			0.173 (1H)		
a(N)	0.663	0.664	0.662	0.675	0.678
			0.669		

a number of organic radicals, two different methods were used for our molecules for optimization of the structures.

The semiempirical AM1 method can be used for a fast calculation of the potential energy surface. Density functional theory (DFT) can be employed with low computational costs and high accuracy for the geometry reoptimization of radicals with more than five heavy atoms [31]. *Becke*'s Three Parameter Hybrid method including the *Lee*, *Yang*, *Perdew* Correlation Functional (*B3LYP*) and the larger contracted *Gaussian* basis set 6-31G* were used in this work.

TMPPD and *DPB* were optimized with the two methods described. The geometries of *TEPPD* and *TPPPD* have been calculated by using the optimized structure of *TMPPD* so that the α-carbons were fixed in the plane of the aromatic ring based on the results of full geometry optimizations of *TMPPD* and *DPB*. The full potential energy surfaces have been investigated using the semiempirical AM1 method for *TEPPD* and *TPPPD*. Reoptimization of the five and nine lowest local minima by the DFT method results then in five and eight minima, which have been included in this study. *Fermi* contact analyses were done for all these minima. For

TiPPPD, the global minimum of *TEPPD* was used as initial structure with an α-hydrogen changed into CH_3. Published optimized geometry of *TMPPD* served as a reference [25, 26].

AM1 calculations were done with the program VAMP [32] for *TEPPD* and *TPPPD*. All other calculations were made with the GAUSSIAN 94 program package [33].

Fermi contacts are obtained in atomic units by GAUSSIAN 94 *via* Eq. (1) [34].

Table 9. Relative AM1 and *B3LYP*/6-31G* energies (in kJ/mol) and hyperfine coupling constants (mT) of the *TPPPD* radical cation; the DFT conformers were used for the *Boltzmann* distribution; the *B3LYP*/6-31G* absolute energy of the global minimum is −814.4968627 a.U.; the dihedral angles A-B of the propyl unit are gauche $g \sim 87$ degree, $g' \sim -87$ degree and trans $t \sim 180$ degree for A (the rotation around the $-CH_2-CH_2$ bond) and gauche, $g \sim 60$ degree, $g' \sim -60$ degree and trans, $t \sim 180$ degree for B (the rotation around the $-CH_2-CH_3$ bond)

Structure	*gt,gt,gt,gt*	*g′t,g′t,gt,gt*	*gg,gt,gt,gt*	*g′g′,g′t,gt,gt*	*g′t,gt,gt,gt*
degeneration	4	2	2	2	2
E_{rel}(AM1)	0.10	0.0	1.42	1.34	1.50
E_{rel}(DFT)	0.0	4.40	4.20	4.32	4.39
Boltzmann distribution	70.6%	6.0%	6.5%	6.2%	6.0%
$a(H_{ar})$	−0.185	−0.177	−0.184	−0.186	−0.178
		−0.193			−0.193
$a(H\alpha)$	0.430 (4H)	0.491 (4H)	0.364 (1H)	0.467 (1H)	0.488 (1H)
	0.316 (4H)	0.270 (4H)	0.357 (1H)	0.303 (1H)	0.256 (1H)
			0.485 (1H)	0.347 (1H)	0.561 (1H)
			0.289 (1H)	0.377 (1H)	0.194 (1H)
			0.439 (2H)	0.445 (2H)	0.436 (2H)
			0.313 (2H)	0.300 (2H)	0.318 (2H)
a(N)	0.664	0.659	0.665	0.663	0.659
		0.668	0.664	0.664	0.668

Structure	*g′g′,g′g′,gt,gt*	*g′g′,g′g′,g′t,g′t*	*g′g′,g′t,gg,gt*	*gt,gg,gg,gt*
degeneration	2	2	2	2
E_{rel}(AM1)	2.60	2.66	2.69	2.74
E_{rel}(DFT)	8.35	8.19	8.57	8.44
Boltzmann distribution	1.2%	1.3%	1.1%	1.1%
$a(H_{ar})$	−0.177	−0.177	−0.185	−0.185
	−0.193	−0.191		
$a(H\alpha)$	0.488 (1H)	0.556 (2H)	0.438 (2H)	0.483 (2H)
	0.255 (1H)	0.215 (2H)	0.292 (2H)	0.292 (2H)
	0.561 (1H)	0.439 (2H)	0.336 (2H)	0.370 (2H)
	0.194 (1H)	0.314 (2H)	0.390 (2H)	0.353 (2H)
	0.439 (2H)			
	0.313 (2H)			
a(N)	0.659	0.662	0.664	0.644
	0.668	0.664		

Table 10. Redox potentials of the first and second oxidation steps of various *p*-phenylenediamines in CH_3CN; supporting electrolyte: 0.1 *M TBAP*; potentials in mV *vs.* Fc/Fc^+ (ferrocene/ferrocenium); UV-VIS data of the semiquinone radical cations in methanol

	$\frac{E_{ox}^{(1)}(R/S^{+\bullet})}{mV}$	$\frac{E_{ox}^{(2)}(S^{+\bullet}/T^{2+})}{mV}$	$\frac{\lambda_{max}(S^{+\bullet})}{nm}$
TMPPD[a]	−280	+295	614, 565, 527 (sh)
TEPPD[a]	−360	+295	611, 561, 526 (sh)
TPPPD	−375	+300	617, 574, 528 (sh)
TiPPPD	−295	+300	617, 574, 528 (sh)
TBzPPD	−120	+525	619, 570, 528 (sh)
DPB	−375	+235	616, 565, 524

[a] From Ref. [42]

$$a_i = 0.28025 \cdot \frac{8\pi}{3h} g_e \beta_e g_N \beta_N \cdot \rho(r_i) \quad (1)$$

$\rho(r_i)$ is the spin density on the nucleus *i*, which is just $\rho(r_i) = |\Psi(r)|^2$, where $\Psi(r)$ is the molecular orbital containing the unpaired electron. g_e and g_N are the electron and nuclear *g*-factors, β_B and β_N are the *Bohr* and nuclear magnetons, respectively. Conversion factors from atomic units to mT are 1595 for hydrogen, 404.3 for nitrogen, and 115.4 for carbon, respectively.

Fermi contacts are also computed with the *B3LYP*/6-31G* method and the more reliable basis set for magnetic properties *B3LYP*/EPR-II. *Boltzmann* distributions were calculated for *TEPPD* and *TPPPD* after degeneration of the local minima to receive the mean computed hyperfine coupling constant for comparison with the experimental values at room temperature. Tables 8 and 9 show the computed hyperfine coupling constants for the local minima of *TEPPD* and *TPPPD*. The *TMPPD* radical cation has been reoptimized with the method described in the *Methods* section, based on published results [25, 26]. The methyl carbon atoms lie in the plane of the aromatic ring. The calculated hyperfine coupling constants are compared with experimental data [12, 35] in Table 1. Although the EPR-II basis set is referred specially for hyperfine coupling constants, the combination of the density functional method using the *B3LYP* functional and the 6-31G* basis set gives hyperfine coupling constants closer to the experimental ESR values. The nitrogen hyperfine coupling constant is calculated around 8% too small, whereas the methyl value is calculated around 5% too large. The aromatic hydrogen couplings constant agree very well with the experimental ones.

For the radical cation of *TEPPD*, 64 local minima are found using the AM1 method, some of them are degenerated. The five energetically lowest conformations with relative energies below 3.26 kJ/mol were then reoptimized with DFT, and lead to a range of relative energies up to 9.36 kJ/mol. After *Fermi* contact analyses the calculated *Boltzmann* weighted coupling-constants are listed in Table 3. Again, the EPR-II coupling constant for nitrogen is ∼20% smaller than the experimental one, whereas the 6-31G* hfc-constant for nitrogen is in good agreement with the experimental value. The hyperfine coupling constants for the aromatic and the α- and the β-hydrogen atoms are in good agreement with the experimental values. The total spin densities for the global minimum are 0.286 on

the nitrogen atoms and 0.093 on the connecting aromatic carbon atoms for all five conformations included.

For the radical cation of *TPPPD* the nine energetically lowest AM1 minima, have relative energies lower than 2.74 kJ/mol (see Table 9). DFT optimization of these nine geometries lead to nine conformations with relative energies lower than 8.57 kJ/mol. *Boltzmann* weighed hfc-constants are listed in Table 3. Because the EPR-II basis set gives hyperfine coupling constants which are around 20% too small for the nitrogen atoms in *TMPPD* and *TEPPD*, only the 6-31G* basis set was used for further investigations. Again the nitrogen hyperfine couplings are around 5% smaller than the experimental values, which show a slight solvent dependence. The hydrogen coupling constants are in good agreement with the experimental data.

For the radical cation of *TiPPPD* the global minimum of *TEPPD* was used to create the starting configuration, which is optimized to an all-trans conformation of all α-hydrogen atoms. The computed *Fermi* contacts are shown in Table 4 and deviate from the experimental α-proton-constants. This leads to the conclusion that our choice of the all-*t* structure is not the most stable conformer in solution.

The radical cations of *TBzPPD* and *BDMAP* have not been included in the computational study. The measured coupling constants are listed in Tables 5 and 7, respectively.

The radical cation of *DPB* was optimized using the *B3LYP*/6-31G* method and it shows the α-carbon atoms of the five-ring in the plane of the benzene ring, whereas the β-carbon atoms lie 5 degree out of plane. The nitrogen *Fermi* contact again gives nitrogen couplings 5% smaller than the experimental ones measured in different solvents (see Table 6).

Conclusion

EPR and ENDOR spectra of the radical cations of six alkyl- and benzyl-substituted *N*,*N*,*N*′,*N*′-*p*-phenylenediamines (*TMPPD-DPB*), together with *N*,*N*′-bis[4-dimethylamino)phenyl]piperazine (*BDMAP*) have been investigated experimentally. Both, EPR and ENDOR spectra are well resolved, not only for the α-hydrogen couplings, but also for the β-hydrogen couplings in *TEPPD-DPB* and even for the γ-hydrogen couplings in *TiPPPD*.

Density functional analyses of the hyperfine coupling constants have been performed for the compounds *TMPPD*, *TEPPD*, *TPPPD*, *TiPPPD* and *DPB*, including *Boltzmann*-weighted conformers for *TEPPD* and *TPPPD* and global or local minima for all other compounds. The computed hyperfine coupling constants are always too small and show deviations from the experimental ones of around 0.01 mT for the α-hydrogen atoms, 0.015 mT for the β-hydrogen atoms ($\sim$5%), and around 0.05 mT ($\sim$8%) for the nitrogen atoms. Such deviations have also been reported for the calculations of other one-electron magnetic properties [35]. The EPR-II basis set, which is reported explicitly for the calculation of hyperfine coupling constants with the *B3LYP* functional, shows a deviation of more than 20% from the experimental values of the nitrogen atoms using our *B3LYP*/6-31G* optimised structures of *TMPPD* and *TEPPD* and was therefore not applied for the larger molecules.

Experimental

^{1}H and ^{13}C NMR spectra were recorded on a Bruker MSL-300 NMR spectrometer. UV-VIS spectra of the radical cations ($S^{+\bullet}$) were obtained by iodine oxidation of the corresponding *p*-phenylenediamine in methanol. The UV-VIS spectra of the neutral compounds (R) were measured in cyclohexane. UV-VIS spectra were recorded either with a Shimadzu-spectrometer UV-3101PC or a Bruins Instruments Omega-10 UV/VIS spectrometer. Melting points were determined using a Büchi melting point apparatus. The reported melting points are uncorrected. A JEOL-ESR X-band spectrometer, type PE-3X (100 kHz field modulation) with microwave preamplification [37] and a temperature control unit JEOL-VT-10 was used to record the CW-ESR spectra (Graz group). The amplified signals were stored via an A/D-interface (BMC, Typ PC20) in a PC. Coupling constants were extracted from the CW-ESR spectra by using the autocorrelation-function procedure [38, 39]. ESR and ENDOR spectra were recorded on a Bruker ER 220D ESR spectrometer equipped with a Bruker ENDOR cavity ER200ENB (Berlin group). For ESR measurements typical experimental conditions were 1.24 or 2 mW microwave power level and 0.01 mT field modulation (12.5 kHz). For ESR saturation and ENDOR measurement a microwave power level of 20 mW was used. The RF power was between 120 and 230 W. FM modulation amplitude was set between $\pm$30 kHz and $\pm$50 kHz, modulation frequency 10 kHz. ESR spectral simulations were performed on a local workstation (SGI Indigo) or on an Pentium PC by means of the programs EPRFT or HFFIT [39]. The Lisbon group used a Bruker ESR spectrometer, type ESP 300 E equipped with an EN 810 ENDOR unit. A conventional three-electrode arrangement was used to get the redox potentials by cyclic voltammetry in CH_3CN. Tetrabutylammonium perchlorate (0.1 *M*) served as supporting electrolyte. Redox potentials and UV-VIS data are listed in Table 10.

N,N,N′,N′-Tetramethyl-p-phenylenediamine (TMPPD)

The compound was purchased from Aldrich and sublimated before use. Completely white crystals have been obtained after several careful sublimations.

N,N,N′,N′-Tetraethyl-p-phenylenediamine (TEPPD)

Freshly distilled *N,N*-diethyl-*p*-phenylenediamine (5.0 g, 30 mmol, Merck, 98%) was dissolved in 75 mmol of a 50% potassium hydroxide solution at elevated temperature. Under nitrogen atmosphere 9.3 g (60 mmol) of distilled diethylsulfate (Fluka, purum, >99%) were added then in drops. After refluxing for another one hour the solution was cooled for two hours. The precipitated product was filtered off, washed with cold argon saturated water, and dried. Additionally the filtrate was extracted with diethyl ether. After drying with anhydrous sodium sulfate (Merck, *p.a.*) the solvent was removed and the residue was purified together with the precipated product by vacuum sublimation to yield bright white crystals. Mp 50°C; ^{1}H NMR (C_6D_6): $\delta = 0.99$ (t, 12H, $J_{H-H} = 7.0$ Hz), 3.05 (q, 8H, $J_{H-H} = 7.1$ Hz), 6.80 (s, 4H) ppm; ^{13}C NMR (C_6D_6): $\delta = 13.3$, 46.4, 117.7, 141.9 ppm; UV-VIS (cyclohexane): $\lambda_{max.}$ (log ε) = 269 (4.161), 321 (shoulder, 3.279) nm.

N,N,N′,N′-Tetra-n-propyl-p-phenylenediamine (TPPPD) [39]

Freshly sublimated *p*-phenylenediamine (4.0 g, 37 mmol, Merck, 99%) and 85.0 g (500 mmol) of distilled *n*-propyliodide (Fluka, purum, >98%) were dissolved in 25 cm^3 of benzene. Then 7.0 g (180 mmol) of sodium amide (Fluka, pract.) were added carefully by small amounts to this solution over a 1 hour period under argon atmosphere. The suspension was stirred for another 2 hours at room temperature and subsequently refluxed for 24 hours. At this stage the course of the reaction could be controlled by applying a simple oxidation reaction to a small sample of the reaction mixture: A few drops of a methanolic iodine solution added to a diluted solution of the sample in methanol should generate the stable radical cation of the product which is easily to be identified by its characteristic

UV-VIS-spectrum ($\lambda_{max.}$ (methanol) = 569, 619 nm). After passing this test positively the solvent and the excess of *n*-propyliodide was removed completely. The dried residue was extracted in a *Soxhlet* extractor with 300 ml of peroxide free diethylether for 4 hours. The solution obtained was washed with argon-saturated water and dried with anhydrous sodium sulfate (*p.a.*). Thereafter the solution was filtered through a layer of neutral aluminum oxide (Fluka, chromatography type 507 C neutral, 100–125 mesh) to remove the coloured side products. Repeated packed column rectification of the crude product *in vacuo* under nitrogen atmosphere yielded a slightly yellowish viscous oil. Bp 150°C (1 mbar); ^{1}H NMR (C_6D_6): $\delta = 0.82$ (t, 12H, $J_{H-H} = 7.5$ Hz), 1.50 (hex, 8H), 3.02 (t, 8H, $J_{H-H} = 7.1$ Hz), 6.80 (s, 4H) ppm; ^{13}C NMR (C_6D_6): $\delta = 12.1$, 21.5, 55.2, 117.4, 142.3 ppm; UV-VIS (cyclohexane): $\lambda_{max.}$ (log ε) = 269 (4.190), 321 (shoulder, 3.267) nm.

N,N,N′,N′-Tetra-isopropyl-p-phenylenediamine (TiPPPD)

Freshly sublimated *p*-phenylenediamine (4.0 g, 37 mmol, Merck, 99%) and 85.0 cm^3 (500 mmol) of redistilled 2-iodopropane (Aldrich, 99%) were dissolved in 25 cm^3 of benzene. Then 7.0 g (180 mmol) of sodium amide (Fluka, pract.) were added carefully and by small amounts to this solution over a 1 hour period under nitrogen atmosphere. The suspension was stirred for 2 hours at room temperature and subsequently refluxed for 48 hours performing the oxidation test from time to time. Realizing that even after such a long time the alkylation process was not completed but came to an end the reaction was stopped. The solvent and the excess of 2-iodopropane were removed completely. The dried residue was extracted in a *Soxhlet* extractor with 300 cm^3 of peroxide free diethyl ether for 4 hours. The solution obtained was washed with argon-saturated water and dried with anhydrous sodium sulfate. The solution was filtered through a layer of neutral aluminum oxide to remove the solvent as well as coloured side products. Packed column rectification of the crude product *in vacuo* under nitrogene atmosphere followed by chromatography on basic aluminum oxide (Fluka, chromatography, type 5016 A basic) using benzene as eluent and controlling the fraction composition by UV-VIS-spectroscopy of the oxidized semiquinonoid radical cation ($\lambda_{max.}$ (methanol) = 574, 617 nm) finally resulted in slightly yellowish crystals. Mp 34.5°C; ^{1}H NMR (C_6D_6): $\delta = 1.06$ (d, 24H, $J_{H-H} = 6.4$ Hz), 3.50 (sept., 4H, $J_{H-H} = 6.4$ Hz), 6.96 (s, 4H) ppm; ^{13}C NMR (C_6D_6): $\delta = 22.1$, 48.9, 125.2, 142.4 ppm; UV-VIS (cyclohexane): $\lambda_{max.}$ (log ε) = 270 (4.093), 314 (shoulder, 3.068) nm.

N,N,N′,N′-Tetrabenzyl-p-phenylenediamine (TBzPPD)

A mixture of 3.0 g (28 mmol) of freshly sublimated *p*-phenylenediamine (Merck, 99%), 12.0 g (113 mmol) of dried anhydrous sodium carbonate (Fluka, puriss. *p.a.*, >99.5%) and 88.0 g (695 mmol) of benzylchloride (Fluka, >99%) was refluxed for 12 hours in a nitrogen atmosphere. An oxidation test (s.a.) was performed to indicate the end of reaction (λ_{max} (methanol) = 570, 619 nm). Excessive benzylchloride was removed completely under reduced pressure and the remaining highly viscous residue was extracted in a *Soxhlet* extractor with 300 cm^3 of tetrahydrofurane. The extract was concentrated and cooled down. The yellow needles precipitated were filtered off and washed carefully with little portions of ice-cold tetrahydrofurane. Purification could be achieved by recrystallization from benzene. Mp 149°C; ^{1}H NMR (C_6D_6): $\delta = 4.27$ (s, 8H), 6.59 (s, 4H), 7.09 (m, 20H) ppm; ^{13}C NMR (CCl_4/D_2O): $\delta = 56.0$, 116.0, 127.8, 129.3, 140.0, 142.8 ppm; UV-VIS (cyclohexane): $\lambda_{max.}$ (log ε) = 265 (4.262), 339 (3.415) nm.

1,4-Dipyrrolidinobenzene (DPB) [36]

Freshly sublimated *p*-phenylenediamine (6.1 g, 56 mmol, Merck, 99%) and 35.0 g (113 mmol) of freshly distilled 1,4-diiodobutane were dissolved in 75 cm^3 of tetrahydrofurane. 24.4 g (230 mmol) of dried anhydrous sodium carbonate (*p.a.*) were added then and the mixture was refluxed for 1 hour

under nitrogen atmosphere. After passing the oxidation test successfully ($\lambda_{max.}$ (methanol) = 524, 565, 616 nm) the solvent was removed completely and the dried residue was dissolved in argon-saturated semi-concentrated hydrochloric acid. The hydrochloric acid solution was neutralized carefully with argon-saturated ammonium hydroxide and the precipitated crude product was collected, washed with cold water, and dried. Subsequently the solid substance was dissolved again in tetrahydrofurane refluxed together with a little amount of activated charcoal (Merck, *p.a.*) under a nitrogen atmosphere and finally hot filtered through a layer of basic aluminum oxide (s.a.) to remove coloured side products. After removal of the solvent under reduced pressure the obtained product was purified by vacuum sublimation to yield bright yellowish needles. Mp 151°C (dec.); ^{1}H NMR (C_6D_6): $\delta = 1.61$ (quin., 8H, $J_{H-H} = 3.3$ Hz), 3.08 (m, 8H), 6.74 (s, 4H) ppm; ^{13}C NMR (C_6D_6): $\delta = 25.8$, 48.9, 114.3, 141.5 ppm; UV-VIS (cyclohexane): $\lambda_{max.}$ (log ε) = 270 (4.520), 342 (3.699) nm.

N,N′-Bis[4-(dimethylamino)phenyl]piperazine (BDMAP) [24]

The synthesis of this compound followed the procedure recently described by *Nelsen et al.* [24].

Radical Generation

For CW-ESR and ENDOR measurements concentrations in the range of 10^{-3}–10^{-4} *M* for the various diamines in a 2-propanol/*DMSO* (dimethylsulfoxide) mixture (1:1 *v*) were used after argon had been bubbled through them for 15 minutes. After addition of a trace of dry silver perchlorate the cation radical emerges spontaneously (Berlin group). The Graz group used methanolic iodine solution ($5 \cdot 10^{-5}$ *M*) to oxidize the corresponding *p*-phenylenediamines ($1 \cdot 10^{-4}$ *M*) in methanol. Oxidation with iodine in a 3:1 *v* mixture of glycerol-water was performed by the Lisbon group for ENDOR-spectra. The CW-ESR spectra were measured in water, there.

It is well established since the early work of *Michaelis* and *Granick* [40], that there exist two well defined oxidation steps for *p*-phenylenediamines. The neutral tetra-substituted *p*-phenylenediamines (*R*) are oxidized by one-electron steps to the corresponding quinoid radical cations ($S^{+\bullet}$) and furthermore to the doubly charged diamagnetic quinonediimines (T^{2+}). The synproportionation equilibrium shown in Eq. (2) is strongly shifted to ($S^{+\bullet}$) in aprotic solvents.

$$2S^{+\bullet} \rightleftharpoons R + T^{2+} \tag{2}$$

This reaction scheme was later extended to *Weitz* and *Wurster* type radicals by *Hünig et al.* [41].

Acknowledgement

G. Grampp and *SL* would like to thank the Austrian Academic Exchange Service (ÖAD), the Volkswagen-Foundation (Germany), and the Austrian Federal Ministery of Education, Science, and Culture for financial support. ERASMUS-SOCRATES scholarships from the EC are gratefully acknowledged by *JPT* and *SL*. *JPT* and *AJSCV* thank for financial support from FCT through its Centro Processos Químicos da Universidade Técnica de Lisboa. *SL* would also like to thank the DFG (Deutsche Forschungsgemeinschaft) for financial support. *AK* would gratefully like to thank *Matthias Hennemann* at the Computer-Chemie-Centrum, University of Erlangen (Germany) for calculating the AM1 geometries of *TEPPD* and *TPPPD*. The authors wish to thank *G. Gescheidt* for helpful discussions.

References

[1] Wurster C, Sendtner R (1879) Ber Dtsch Chem Ges **12**: 1803
[2] Weitz E, Fischer K (1925) Angew Chem **38**: 1100
[3] James TH (ed) (1977) The Theory of the Photographic Process. New York

[4] Weissman SI, Townsend J, Paul DE, Pake GE (1953) J Chem Phys **21**: 2227
[5] Chu TL, Pake GE, Paul DE, Townsend J, Weissman SI (1953) J Phys Chem **57**: 504
[6] Lipkis D, Paul DE, Townsend J, Weissman SI (1953) Science **117**: 534
[7] Hausser KH (1960) Naturwiss **47**: 152
[8] Hausser KH (1963) Mol Phys **7**: 195
[9] Bolton JR, Carrington A, dos Santos-Veiga J (1962) Mol Phys **5**: 615
[10] Weil JA, Bolton JR, Wertz JE (1994) Electron Paramagnetic Resonance. Wiley, New York, p 512
[11] Knolle WR (1970) PhD Thesis, University of Minnesota, Minneapolis, MN
[12] Grampp G, Stiegler G (1984) Z Phys Chem NF **141**: 185
[13] Weissman SI (1954) J Chem Phys **22**: 1135
[14] McLachlan AD (1958) Mol Phys **1**: 233
[15] Latta BM, Taft RW (1967) J Am Chem Soc **89**: 5172
[16] Yao T, Musha S (1974) Chem Lett 939
[17] Allendoerfer RD, Rieger PH (1966) J Am Chem Soc **88**: 3711
[18] Bullock AT, Howard CB (1977) J Magn Res **25**: 47
[19] Horsman G (1967) Coll Ampere **XIV**: 578
[20] Zhang F, Zhonli G, Liu Chem Y (1988) J Chinese Univ **4**: 24
[21] Telo JP, Dias RMB, Vieira AJSC (1995) 2° Congresso de radicais livres em Química, Biologia e Medicina. Porto, Portugal
[22] Truchin MI (1976) Leningradskij institut jadernoj fizihi, B.P. Kostantinova (translated by Technical Information Libery, Hannover/Germany) **273**: 2; Truchin MI (1976) Academy of Sciences of USSR, Leningrad, Institute of Nuclear Physics **273**: 2
[23] Marken F, Webster RD, Bull SD, Davies SG (1997) J Electroanal Chem **437**: 209
[24] Nelsen SF, Yunta MJR (1994) J Phys Org Chem **7**: 55
[25] Brouwers AM (1997) J Phys Chem A **101**: 3626
[26] Rauhut G, Clark T (1993) J Am Chem Soc **115**: 9127
[27] McKinney TM, Geske DH (1967) J Am Chem Soc **89**: 2806
[28] Bock H, Vanpel T, Näther C, Ruppert K, Havlas Z (1992) Angew Chem **104**: 348
[29] Kurreck H, Kirste B, Lubitz W (1984) Angew Chem **96**: 171
[30] Kurreck H, Kirste B, Lubitz W (1988) Electron Nuclear Double Resonance Spectroscopy of Radicals in Solution. VCH, Weinheim
[31] Batra R, Giese B, Spichty M, Gescheidt G, Houk KN (1996) J Phys Chem **100**: 18371
[32] Clark T, Alex A, Beck B, Chandrasekhar J, Gedeck P, Horn A, Hutter M, Rauhut G, Sauer W, Steinke T (1998) F90VAMP, Version 7.0 alpha, Erlangen
[33] Frisch ME, Trucks GW, Schlegel HB, Gill PMW, Johnson BG, Robb MA, Cheeseman JR, Keith T, Petersson GA, Montgomery JA, Raghavachari K, Al-Laham MA, Zakrzewski VG, Ortiz JV, Foresman JB, Cioslowski J, Stefanov BB, Nanayakkara A, Challacombe M, Peng CY, Ayala PY, Chen W, Wong MW, Andres JL, Binkley JS, Defrees DJ, Baker J, Stewart JP, Head-Gordon M, Gonzalez C, Pople JA (1995) Gaussian 94, Revision E.1, Gaussian, Inc., Pittburgh PA
[34] Schlegel HB (1995) Exploring Chemistry with Electronic Structure Methods. Gaussian, Inc., Pittsburgh PA
[35] Kaupp M, University of Würzburg, Germany (personal communication)
[36] Vieira AJSC, Universidade de Nova Lisboa, Portugal (personal communication)
[37] Grampp G (1985) Rev Sci Instrum **56**: 2050
[38] Grampp G, Schiller CA (1981) Anal Chem **53**: 560
[39] Kirste B (1992) Anal Chim Acta **365**: 191
[40] Michaelis L, Granick S (1943) J Am Chem Soc **65**: 1747
[41] Deuchert K, Hünig S (1978) Angew Chem **90**: 927
[42] Grampp G, Pluschke P (1987) Coll Czech Chem Commun **52**: 819